

5-2020

Impacts of Spatial and Temporal Variation on the Benthic Nitrogen Cycle in the York River Estuary

Evan Lawrence
William & Mary

Follow this and additional works at: <https://scholarworks.wm.edu/honorstheses>



Part of the [Biochemistry Commons](#), [Marine Biology Commons](#), and the [Systems Biology Commons](#)

Recommended Citation

Lawrence, Evan, "Impacts of Spatial and Temporal Variation on the Benthic Nitrogen Cycle in the York River Estuary" (2020). *Undergraduate Honors Theses*. Paper 1573.
<https://scholarworks.wm.edu/honorstheses/1573>

This Honors Thesis is brought to you for free and open access by the Theses, Dissertations, & Master Projects at W&M ScholarWorks. It has been accepted for inclusion in Undergraduate Honors Theses by an authorized administrator of W&M ScholarWorks. For more information, please contact scholarworks@wm.edu.

Impacts of Spatial and Temporal Variation on the Benthic Nitrogen Cycle in the York River
Estuary


A thesis submitted in partial fulfillment of the requirement
for the degree of Bachelor of Science in Biology from

The College of William and Mary

by
Evan Lawrence

Accepted for _____ Honors _____


Iris Anderson, Advisor


Mark Brush


Doug DeBerry


Rachel O'Brien

Williamsburg, VA
May 6, 2020

Table of Contents:

Abstract	3
Acknowledgements	4
Introduction	5
Methods	8
Results	14
Discussion	19
References	24
Tables and Figures	26

Abstract:

Changing the nitrogen and organic matter (OM) load of a marine ecosystem can dramatically alter its function. Tight benthic-pelagic coupling is a key characteristic of shallow microtidal systems like the York River Estuary (YRE), VA, where ammonification due to remineralization of OM or ammonium uptake during photosynthesis by microphytobenthos (MPB) on the benthic surface can be significant sources, or sinks, for inorganic and organic nitrogen. To examine how benthic nitrogen fluxes vary spatially and temporally in the YRE, as well as to determine the relative importance of the various nitrogen transformations taking place in the estuary, a series of field samplings and laboratory incubations were performed. Remineralization was found to increase with sediment organic content and warmer temperatures, suggesting that organic matter entering the YRE from its watershed or produced in the estuary by primary production drives the benthic nitrogen cycle. Benthic uptake was not a significant sink of ammonium, with most of the NH_4^+ produced in the benthos fluxing into the water column. Nevertheless, benthic uptake displayed variation between stations. Finally, nitrification was a more important sink of ammonium than uptake by the MPB.

Acknowledgements:

First and foremost would like to thank my advisor, Dr. Iris Anderson, for giving me the opportunity and support to do this research. I would also like to thank Hunter Walker, Michelle Woods, Sam Fortin, and Derek Detweiler for putting up with me and for helping greatly in lab and field work. I would like to thank the National Science Foundation for supporting the LYRE project, and all my family and friends who helped me complete this project through moral or editorial support.

Introduction:

In aquatic systems like the York River Estuary (YRE), available nitrogen commonly limits primary production (Mortazavi et al. 2012). Increases to the nitrogen load can shift the metabolism of a system from net heterotrophic to net autotrophic and lead to eutrophication (Anderson et al. 2013). In the YRE, nitrogen additions may also control the appearance of seasonal intense phytoplankton and harmful algal blooms, which in turn contribute to loss of ecosystem services and to hypoxic zones as they sink and decompose. A similar cascade likely occurs in many other shallow microtidal estuaries, which comprise nearly half of estuarine surface area in the U.S. (NOAA (National Oceanic and Atmospheric Administration) 2011). The main source, 90%, of the nitrogen load to the YRE is its watershed (LYRE Annual Report 2019), which is dominated by forest. Runoff from the surrounding 6,900 km² drains into the estuary, impacting the water quality of both the YRE and the Chesapeake Bay (Reay 2009).

Besides terrestrial sources, microbial processes in the estuary itself could potentially account for a significant portion of the ammonium in the YRE (Rizzo 1990). There are two ways for ammonification, the transformation of various forms of nitrogen into ammonium, to take place. Particulate and dissolved organic matter in the system can be converted to ammonium via remineralization. This is a microbial process wherein organic matter is broken down releasing NH_4^+ . Remineralization is commonly limited by the availability of labile organic matter (Tobias et al. 2001). Alternatively, microbes can produce NH_4^+ from NO_3^- through dissimilatory nitrate reduction to ammonium (DNRA), a microbial process, which only occurs under anoxic conditions, whereas remineralization can be either aerobic or anaerobic (Brandes et al. 2007).

Both processes can occur with or without light, although DNRA may be inhibited in the light by algal oxygen production.

While NH_4^+ is produced in both the benthic and pelagic zones, this study focused only on benthic fluxes. It has been estimated that on an annual basis remineralization may be responsible for as much as 10% of the dissolved inorganic nitrogen in the YRE (LYRE Annual Report 2019); however, this is likely an underestimate since it ignores bloom conditions and seasonal variations such as drought and high temperatures. In the New River estuary of North Carolina, benthic remineralization produced a sufficient amount of ammonium to support summer phytoplankton blooms, especially during low precipitation years (Anderson et al, 2013). Once produced, NH_4^+ can experience a number of fates. Most simply, it can flux to the water column where it may fuel primary production, be removed by nitrification, or be taken up by the microphytobenthos (MPB) at the benthic surface during photosynthesis.

Nitrification is a process whereby NH_4^+ is oxidized to NO_2^- and NO_3^- . This microbial process requires oxygen and is limited by either NH_4^+ or O_2 availability (Tobias et al. 2001). Nitrification can lead to a number of outcomes. NO_3^- can undergo microbial denitrification, an anoxic process, which effectively removes $\text{NO}_3^- + \text{NO}_2^-$ (NO_x) from the system as N_2 , a form of nitrogen which is not readily bioavailable (Mortazavi et al. 2012). The rate at which this occurs is directly related to NO_3^- input (Tobias et al. 2001). Alternatively, NO_3^- can be converted back to NH_4^+ through DNRA, or flux out of the sediment into the water column.

If the sediment surface is photic, NH_4^+ can be taken up by the MPB. In this way, ammonium is incorporated into organismal biomass and prevented from reaching the overlying water. This ‘benthic cap’ can be highly effective. Anderson et al. (2013) found that it “removed

from 15 to 137 % of ammonified N^o in the New River Estuary, NC, a shallow estuarine system like the YRE. Under ammonium-limited conditions, MPB may decrease nitrification rates by outcompeting nitrifying microbes for available NH₄⁺; however, by exuding extrapolymeric substances they may also provide microbes with substrate and oxygen to fuel their metabolism (Anderson et al. 2013, Smith et al. 2000, & Tobias et al. 2001).

The relative importance and rates of these processes are controlled by a number of factors. With respect to the YRE I hypothesized that:

1. Gross ammonification rates will vary by location.

Gross remineralization rates are expected to increase towards the head of the estuary, which receives the highest input of particulate and dissolved organic matter from the watershed (LYRE Annual Report 2018). Stations at the head of the estuary will also have higher concentrations of more reactive organic matter, which can fuel high rates of remineralization, and longer residence times (approximately 2 months), compared to stations closer to the mouth (LYRE Annual Report 2019 & Friedrichs 2009). Additionally, remineralization rates are expected to be highest in channel stations where OM may become trapped rather than continuing downstream (Friedrichs 2009).

2. Ammonification and ammonium consumption will vary seasonally.

In the summer and fall, higher temperatures will increase both ammonification and ammonium consumption rates. Besides the effect of temperature on microbial metabolism, warmer temperatures lead to increased stratification and less water column mixing.

3. Ammonium consumption by the MPB will be highest at shoal stations and increase going down estuary.

As opposed to autotrophs that sink to the benthos at channel stations, the MPB are held to the surface of the benthos by exuded extracellular polysaccharides. Accordingly, the MPB should have increased access to light at shoal stations, allowing them to survive and grow and leading to greater ammonium uptake at shoal stations. This increased uptake by the MPB towards the mouth of the YRE will likely disappear up estuary due to more shading from colored dissolved organic matter (CDOM) and total suspended solids.

4. Reduction of ammonium concentrations by nitrification will be highest up estuary during warm months and at channel stations.

Nitrification rates will be highest when the nitrifying microbes do not have to compete with the MPB for substrate. This condition may be met at locations where the benthos is rich in organic matter, in which case NH_4^+ would not be limiting or in aphotic channel stations. Nitrification will also be highest in warm months due to higher metabolic rates among the nitrifying microbes.

5. Gross mineralization will exceed net mineralization when either MPB uptake or nitrification are important NH_4^+ removal processes.

Methods:

Study Site

The York River Estuary is a shallow microtidal tributary of the Chesapeake Bay that comprises the study area and stretches from the confluence of the Mattaponi and Pamunkey Rivers (the two main tributaries of the YRE) at West Point, 52km downstream to the mouth of the river (Reay 2009). Approximately 38% of the total bottom area in the YRE is shallower than 2m and typically receives light (Rizzo 1990). However, there is also a channel, varying in depth from 20m at the mouth of the estuary to 6m at the head (Friedrichs 2009). As of 2009, the

watershed was composed of 61% forest, 21% agricultural lands, 8% water, 7% wetlands, 2% developed lands, and 1% barren lands (Reay 2009).

Agricultural runoff from the watershed is likely a large source of nutrients to the YRE. Sin et al. (2001) found that river discharge into the YRE appeared to be the major factor controlling blooms. Countway et al. (2006) found that there was a significant increase in the OM content of the surface water going up river following high discharge. Additionally, mixing of the water column and nutrient resuspension enhances phytoplankton growth in the water column (Haas et al. 1981). Due to a combination of mixing and sediment input, the turbidity maximum in the YRE is situated near West Point, although it may shift seasonally (Reay 2009). While the YRE commonly experiences large algal blooms, none were recorded during the study periods of October 2019 and January 2020.

Experimental Design

This study was composed of measurements of net and gross benthic NH_4^+ fluxes in sediment cores performed during October 2019 and January 2020. Rates of net ammonium fluxes were determined by sampling overlying water from benthic cores during incubations at ambient temperatures in both the light and dark in an environmental chamber. Gross ammonium flux was measured by the isotope pool dilution technique (Anderson et al, 1997) as the difference in ^{15}N isotope concentrations in extracted NH_4^+ between T initial and T final benthic cores. Gross flux numbers reflect total ammonification rates; the variation between the net and gross fluxes reflect sediment NH_4^+ consumption, and the difference between net fluxes in the dark and light indicates uptake by the MPB. To detect spatial and temporal variations, samples were taken from each of five sampling regions from down to up estuary, and at two time points three months

apart. Extra cores at each station were taken to quantify percent organic content and sediment chlorophyll *a* concentration.

Core Collection

Cores for the incubation experiments were taken in October 2019 and January 2020. In October, cores were taken at each of five shoal sampling stations, located within 5 boxes along the YRE salinity gradient, numbered 2, 3, 5, 8, and 9 (station numbers increase going up estuary, Fig. 1). In January, cores were taken from both shoal and channel stations of every other box, shoal stations 2, 5, and 9, and channel stations 1, 6, and 10. These channel stations were added in January to investigate variation in NH_4^+ fluxes by depth.

All shoal cores were taken by hand with pole corers, while channel cores were taken using a box grab sampler. Only sediment samples where the top layer of the benthos remained intact were used. Cores for the gross flux experiments were collected in plexiglass tubes 5.7 cm in diameter and 10 cm tall. The bottom 4 cm of each of these cores had 16 small holes, 4 rows of 4 holes, which were spaced equidistantly along the height and circumference of the cores. These holes allowed for the homogeneous injection of ^{15}N into samples. The openings were filled with silicon prior to collection to prevent leakage. Once cores were taken, sediment heights of all gross flux cores were standardized to 4 cm by removing sediment from the bottom of the cores. Six cores were taken from each station in order to measure both T_0 and T_F ammonium concentrations and $^{15}\text{N}\text{-NH}_4^+$ atom % enrichment in triplicate.

Net flux cores were 6 cm by 29 cm and collected in the same manner. These cores were taken to a depth of approximately 10 cm. Triplicate net cores were collected at each station along with one additional core for sediment characterization. The headspace of each core was filled

with filtered (1 μm) site water from the depth at which they were taken. Cores were capped and placed in a cooler with ice for transport back to the lab.

Triplicate benthic chlorophyll *a* samples were taken at each station using a syringe with the tip removed. Samples were sectioned (0 – 1 cm) into exetainer tubes and transported to the lab in a cooler. Additional water for use in flux experiments was taken from depths directly above the bottom at each site. Water samples were transported in opaque containers or covered with trash bags to prevent light from altering water chemistry.

At the lab, all cores were unloaded, uncapped, and separated by station into buckets of unfiltered, or 1 μm -filtered for channel stations, site water. Bubblers were added to these buckets to circulate and aerate the water, and all buckets were placed in a dark environmental chamber set to *in situ* YRE water temperatures. Cores were left to equilibrate overnight.

Gross Flux Incubations

Gross fluxes were measured using the isotope pool dilution method (Anderson et al. 1997). The morning after sampling, gross flux cores were removed from their buckets to start the experiment. Three T_0 cores per station were randomly selected and processed first. The overlying water was siphoned off, leaving just enough to prevent disturbing the sediment, and the sediment was emptied into bags containing 204 ml (twice the volume of the sediment) of 2M KCl for extraction, and 1.6 ml of $(^{15}\text{NH}_4^+)_2\text{SO}_4$ (30 at%, 10mM) to track $^{14}\text{NH}_4^+$ production and dilution of the added $^{15}\text{NH}_4^+$ in the T_0 cores. These samples were then shaken for an hour and frozen until they could be analyzed.

The remaining cores were drained and injected with 0.1 ml of $(^{15}\text{NH}_4^+)_2\text{SO}_4$ (30 at%, 10mM) per hole using 1.5 cm long needles to ensure homogenous distribution. Then the core

headspaces were refilled with filtered (1 μm) site water, a magnetic stir bar was added to ensure water circulation, and cores were recapped and placed in a dark incubator set to *in situ* water temperature. After a 24 hour incubation period, the overlying water was drained and the sediment was put into bags containing 204 ml 2M KCl, shaken for an hour, and then frozen.

To prepare for analyses sediment bags were thawed, and 50ml of slurried sediment were collected from each bag and centrifuged for 5 minutes at 5000 rpm to pelletize the suspended sediment. Centrifuged samples were filtered through a 0.45 μm polyethersulfone filter into two exetainers, one for dissolved inorganic nitrogen (DIN) analysis and one for ^{15}N analysis by membrane inlet mass spectrometry (MIMS). These were stored in water and refrigerated for no more than a week until analysis took place. At this stage salinities of each sample were also taken to calculate gas constants.

Net Flux Incubations

Net flux incubations were conducted the morning after collection. Cores were removed from their buckets and the overlying water was carefully drained to avoid disturbing the surface sediment. Site water, which had been filter-sterilized through 0.2 μm polyethersulfone filters, was then used to refill the cores. A magnetic stir bar was added to each core, and they were recapped and replaced in their respective buckets, along with a core containing only filtered site water to act as a control.

All cores were sampled every 45 minutes over the course of a seven hour incubation, three hours in the dark followed by an hour transition to the light and an additional three hours in the light. This sampling consisted of measuring dissolved oxygen (DO) levels with a PreSens, Fibox 4 oxygen sensing system with flow-through cell and removal of 10-15ml of

water for DIN analysis. The water samples were filtered through 0.45 μm polyethersulfone filters and frozen until analysis. The water removed from the cores was replaced from carboys of filter-sterilized site water connected to the cores. Water samples at the start and end of the incubation were also taken from these carboys to correct for any change in DIN concentrations.

Net NH_4^+ Fluxes

Ammonium concentrations in samples taken from the net flux incubations were measured using a Lachat QuickChem 8000 Auto Analyzer. Net NH_4^+ fluxes in the light and dark incubations were calculated from the DIN concentration results as:

$$\text{Hourly Flux} = (m \times V)/A$$

$$\text{Daily Flux} = (F_l \times h_l) + (F_d \times h_d)$$

where m is equal to the slope of the linear regression of concentration (mM) versus time (hours); V is equal to the volume of overlying water in the flux core (liters); A is the sediment surface area within the core (m^2); F_d and F_l are hourly fluxes in the dark and light, respectively ($\text{mmol m}^{-2} \text{h}^{-1}$), and h_d and h_l are the number of hours of dark and light in a day, respectively. For comparison, these were converted into rates of $\text{mmol m}^{-2} \text{d}^{-1}$.

Gross N Mineralization

For isotope analysis by MIMS, NH_4^+ in the samples was first oxidized to N_2 by the OX/MIMS method, using hypobromite as described by Yin et al. (2014). Then the samples were analyzed for $^{29}\text{N}_2$ and $^{30}\text{N}_2$ using a MIMS equipped with a copper column inside a 600 $^\circ\text{C}$ furnace. To account for variation, three measurements from each sample were averaged and the results were corrected for drift. Total $^{15}\text{NH}_4^+$ enrichment in gross flux cores was calculated using MIMS measurements as:

$$^{15}\text{NH}_4^+ \text{ enrichment} = (^{29}\text{N} + 2 * ^{30}\text{N}) / (2 * (^{28}\text{N} + ^{29}\text{N} + ^{30}\text{N}))$$

where ^{28}N , ^{29}N , and ^{30}N are equal to the % enrichment of each of these isotopes.

Concentrations of ammonium in gross flux cores were measured in the same manner as for net incubations. Gross ammonification was then calculated using a model described by Wessel et al. (1992) as:

$$\text{Ammonification} = \frac{\ln (T_{f_{\text{atm}\%}} - k) / (T_{0_{\text{atm}\%}} - k)}{\ln [\text{NH}_4^+ T_f] / [\text{NH}_4^+ T_0]} * \frac{[\text{NH}_4^+ T_0] - [\text{NH}_4^+ T_f]}{\text{time}}$$

where $T_{f_{\text{atm}\%}}$ and $T_{0_{\text{atm}\%}}$ refer to the atom % $^{15}\text{NH}_4^+$ enrichment of the T_f and T_0 cores, respectively; k is equal to natural abundance of $^{15}\text{NH}_4^+$ expressed as atom %; $[\text{NH}_4^+ T_f]$ and $[\text{NH}_4^+ T_0]$ are the concentrations of ammonium in the T_f and T_0 cores, respectively, and time is the incubation time (Murphy et al. 2016). These were also converted into rates of $\text{mmol m}^{-2} \text{d}^{-1}$.

Sediment Characterization

Sediment characterization cores were taken to determine percent organic composition of the sediment at each site and to quantify benthic chlorophyll *a*. To determine percent OM, three subsamples of each core were taken to a depth of 1 cm and desiccated in a drying oven. Once dry, these sections were weighed, combusted (500°C for 4 hours), and reweighed. Percent organic matter was calculated as:

$$\text{Percent organic matter} = (\text{ash free dry weight g/dry weight g}) * 100$$

Sediment chlorophyll *a* samples in triplicate cores were stored frozen at -15°C until extraction in 10 mL of a solution of 90% acetone in deionized water. Samples were then vortexed and sonicated for 30 s and stored frozen for 24–28 h before filtration (Pall Acrodisc CR

0.45 μm PTFE membrane) and analysis on a spectrophotometer (model DU800, Beckman Coulter, Inc., Brea, CA, USA) (Anderson et al, 2013). Chlorophyll *a* concentrations (mg/m^2) were calculated according to the equations in Lorenzen (1967).

Statistical Testing

All paired t-tests and ANOVAs in this study were performed in RStudio version 1.2.5042, and all linear regressions were performed using Microsoft Excel version 16.30.

Results:

Sediment % Organic Matter

In October, sediment percent organic matter varied from 1.42% at shoal station 3 to 13.41% at shoal station 9 (Figure 2). In January it varied from a low of 0.98% at shoal station 5 to a high of 12.4% at shoal station 9. Separated by month, the average percent organic content was 5.0% with a standard error (SE) of 2.2% in October and 5.9% with a SE of 2.0% in January. It is worth noting that all sites sampled in October were shoal stations, while in January both channel and shoal stations were sampled, which prevents the direct comparison of these averages.

Paired t-tests were conducted by month and depth of % sediment organic matter (OM). For monthly comparisons, only data from stations sampled during both January and October, stations 2, 5, and 9, were used (Figure 3). The mean difference between January and October was -1.54%, showing significantly higher ($p=0.05$) sediment organic content in October. To test the relationship between depth and organic content, channel and shoal stations from January were similarly paired by box (Figure 4). A difference of 2.2% suggested higher but not significant ($p=0.58$) % organic matter in channel stations (Table 1).

A one-way ANOVA was performed on shoal stations 2, 5, and 9 from both months grouped by box (Figure 5) to determine the impact of location on %OM. Results showed significantly lower %OM (both with p-values 0.005) in the down-estuary stations, boxes 1 and 3, compared to the up-estuary stations in box 5. Between boxes 5 and 1, the 95% confidence interval showed a range of increase from 6.3 to 15.9 percentage points, and between boxes 5 and 3 from 6.0 to 15.6 percentage points. Boxes 1 and 3 were not significantly different from each other, with a p-value of 0.96 (Table 2).

Benthic Chlorophyll *a*

ANOVA and paired t-tests were performed on benthic chlorophyll *a* data, reported in mg/m², to determine how it was affected by time of year, site depth and estuarine position (Figure 6). Between January and October; the mean of the differences was -57.74 mg/m², suggesting higher chlorophyll *a* in October, but with a p-value of 0.14, this relationship was not significant (Figure 7). Similarly, chlorophyll *a* between channel and shoal stations was not found to differ significantly, with a p-value of 0.59 (Table 3). As seen in Figure 8, stations in box 1, closest to the mouth of the YRE, have the highest density of chlorophyll *a*, but no variation in chlorophyll *a* between any of the boxes was found to be significant (Table 4).

Linear regressions were performed comparing MPB uptake, calculated as the difference between net fluxes in the dark and the light, to benthic chlorophyll *a* by station (Figure 9). With all stations from both months included, the slope of the regression was positive with an equation of $y = 0.06x - 3.80$ and an R^2 of 0.10. However, when calculated based only on January data, the slope was negative, with an equation $y = -0.12x - 0.42$ and $R^2 = 0.05$, whereas when calculated from October data the slope was positive, with equation $y = 0.03x - 0.29$ and $R^2 = 0.15$ (Table 5).

Initial Sediment Ammonium Concentrations

Initial sediment ammonium concentrations in 4 cm deep cores, in mmol/m², (Figure 10) were determined in the T0 gross flux cores. ANOVA and paired t-tests were performed on these data using the same independent variables as for %OM content; linear regressions of sediment ammonium vs. %OM content were also performed. Ammonium concentrations were shown to be significantly higher at channel than shoal stations, with a mean of the differences of 15.18 mmol/m² and p-value of 0.03; seasonal variation was not significant, p-value of 0.52 (Figures 11 & 12, Table 6). Furthermore, concentrations at stations in box 5, top of the YRE, were significantly higher than those in the two lower estuarine boxes. Confidence intervals (95%) showed increases of 0.64-17.1 mmol/m² and 2.1-18.5 mmol/m² between boxes 5 and 1 and 5 and 3, respectively. Concentrations between the lower two boxes were not significantly different (Figure 13 & Table 7).

Linear regressions were performed for each month individually and both months combined between initial sediment NH₄⁺ and sediment organic matter content (Figure 14). The equations of the trendlines showed consistently positive correlations between the variables, with formulas $y = 1.68x + 6.99$ for January, $1.48x + 3.20$ for October, and $y = 1.65x + 4.97$ for both months combined. R² values for these regressions were 0.32, 0.94, and 0.42, respectively (Table 8).

Net Ammonium Fluxes

The same independent variables used for %OM content were used in ANOVA and paired t-tests of net ammonium fluxes, with the addition of paired t-tests comparing net light with net dark fluxes as a whole and by month (Figures 15 & 16). For all tests other than these dark/light

flux comparisons, an integrated daily net flux number was used, calculated by multiplying hourly light and dark flux numbers by the daily hours of light and dark the York River experienced at the time of their collection.

Net ammonium fluxes were significantly higher in January than October with a $4.44 \text{ mmol m}^{-2} \text{ d}^{-1}$ mean of the differences and a p-value of 0.037 (Figure 17 & Table 9). Likewise net fluxes in the channel were significantly higher than those at shoal stations, with a mean of the differences of $15.53 \text{ mmol m}^{-2} \text{ d}^{-1}$ and p-value of 0.049 (Figure 18 & Table 9). However, despite a consistent increase going up estuary, variation between boxes was not significant (Figure 19 & Table 10).

In October, net fluxes were higher in the dark, while in January and both months combined, net fluxes were higher in the light. None of these differences were significant, with p-values of 0.50, 0.12, and 0.21 respectively (Table 9).

Gross Ammonium Fluxes

Finally, the same tests done for %OM content were repeated for gross ammonium fluxes (Figure 20). Additionally, gross fluxes were compared with net fluxes as a whole and by month (Table 12). Gross fluxes were not significantly different between months, with a p-value of 0.41, although October fluxes were higher on average, with a mean of the differences of $-3.8 \text{ mmol m}^{-2} \text{ d}^{-1}$ (Figure 21). Furthermore, gross fluxes did not differ significantly between channel and shoal stations (p-value = 0.33), although channel fluxes were higher on average (mean of the differences $4.21 \text{ mmol m}^{-2} \text{ d}^{-1}$) (Figure 22). Despite showing increases going up estuary, differences in gross fluxes by box were not significant (Figure 23 & Table 11).

Gross and net fluxes were compared against one another using a paired t-test, where samples were grouped by station (Figures 24 & 25). With p-values of 0.46 for October, 0.051 for January, and 0.61 for both months combined, none of these differences were significant. However, in all comparisons, the mean of differences showed gross fluxes to be greater than net fluxes by 2.1, 10.5, and 1.4 mmol m⁻² d⁻¹ for October, January, and both months combined, respectively (Figure 26 & Table 12).

In order to determine whether sediment %OM content correlated with gross fluxes, a linear regression was run between these variables for each month individually, and both months combined (Figure 27). The slope of the line of best fit was positive for each of these comparisons, indicating a direct correlation. The equation of the lines of best fit were $y = 0.46x + 0.40$ for January, $y = 0.63x + 0.50$ for October, and $y = 0.52x + 0.50$ for both months combined. October not only had the steepest slope, but also the highest R² value (0.65). The other regressions had an R² of 0.25 and 0.36, for January and both months combined respectively (Table 13).

Discussion:

The main conclusions to be drawn from this study are that:

1. Ammonium production in the benthos of the YRE is driven by organic matter concentrations.
2. Neither MPB nor nitrifying bacteria remove a significant portion of ammonium production.
3. Nitrification, rather than MPB uptake, is the dominant ammonium removal process.

Net ammonium fluxes were not significantly different from gross ammonium fluxes in either month (Table 12). This suggests that most of the ammonium produced by ammonification fluxed to the water column rather than being taken up by the MPB or nitrifying microbes. However, in calculating daily net ammonium fluxes by extrapolating linearly from 7 hour incubations, this study may have overestimated net ammonium fluxes, thereby minimizing any differences between gross and net fluxes. Ammonium flux rates typically reach an asymptote as labile organic matter becomes limiting during the incubation, and the fluxes level out. Evidently, the incubations in this study did not last long enough to reach this point.

Nevertheless, net fluxes were on average lower than gross fluxes which suggests some ammonium uptake (Table 12). There was a lot of variation between sites and, at many stations, ammonium was released in gross fluxes but taken up in net fluxes (Figure 24 & 25T). Since net fluxes in the light were not significantly different from net fluxes in the dark, most of this uptake was likely due to nitrification rather than MPB uptake (Table 9). The ammonium taken up by MPB varied positively with chlorophyll *a* concentrations. MPB uptake vs. chlorophyll *a* concentration was most closely coupled in October when only shoal stations were sampled (Figure 9 & Table 5). This suggests that, while channel stations may have higher concentrations of chlorophyll *a*, as shown in Figure 4, a large proportion of this chlorophyll could have come from algal cells or detrital material that have sedimented out of the water column rather than active MPB. This could lead to lower ammonium uptake despite higher chlorophyll *a* concentrations.

Benthic chlorophyll *a* distribution did not show any significant variability along the temporal and spatial gradients that were tested (Table 3). Nevertheless, the directionality of the

variance was mostly as expected, suggesting that sample size may have been too small to detect any significant difference. Chlorophyll *a* concentrations varied by estuarine position. Stations at the mouth of the estuary, in box 1, had significantly higher chlorophyll *a* concentrations than stations up estuary, in boxes 3 and 5 (Table 4). This gradient indicates that light likely limits the growth of the MPB, despite higher ammonium concentrations providing more favorable growth conditions up estuary.

Gross fluxes increased going up estuary (Table 11). This is likely due to higher organic matter concentrations at the head of the estuary providing increased substrate for remineralization. As shown in Figure 27, gross ammonium fluxes correlated positively with sediment % organic content, and % organic content was significantly higher in box 5 at the head of the estuary than in boxes 1 and 3 (Table 2). The large decline in organic content from box 5 to box 3 coupled with the nonsignificant differences between boxes 1 and 3, suggest that most of the organic matter entering the estuary from the watershed is rapidly decomposed before it can reach the lower boxes (Figure 5).

The strong correlation between initial ammonium and % OM content suggests that most of the ammonium in the sediment was produced by remineralization of the OM reaching the benthos. Alternatively, high water column ammonium transported into the estuary from the watershed may have influenced the sediment NH_4^+ concentrations. This study found high levels of correlation between initial ammonium and % organic matter content, shown in Figure 14. In October, change in % organic content explained 94% of the variation in initial ammonium concentrations (Table 8). This correlation was not as strong in January, probably because the January sampling period included both channel and shoal stations which introduced another level

of variation into this relationship. Additionally, colder temperatures in January would have reduced OM decomposition rates.

Initial ammonium concentrations varied spatially and temporally in the YRE. They were significantly higher at channel stations than shoal stations, where organic matter can accumulate due to aggregation and less resuspension (Table 6). Ammonium concentrations were also greatest in box 5, at the head of the estuary, where organic matter concentrations, gross fluxes, and net fluxes were all highest (Table 7).

Overall, these correlations suggest that ammonification rates, and thus fluxes of NH_4^+ to the water column, are controlled primarily by organic matter availability. Since much of this organic matter is terrestrial in origin, land use in the watershed of the YRE and freshwater inputs may ultimately control the recycled nitrogen load of the YRE and, in turn, its metabolic state.

Future Directions

This study was originally intended to incorporate data from four sampling periods, one in each season, in order to determine how ammonification and ammonium consumption vary throughout the year. Unfortunately, due to weather conditions that prevented sampling in August 2019, and the COVID-19 pandemic, only two time periods were sampled. Replicating this study as designed would provide a better understanding of benthic nitrogen fluxes in the YRE. Since a bloom would likely disrupt the observed gradients and drastically increase resource patchiness, intensive monitoring during algal blooms would be an important addition to future studies. This could also demonstrate the impacts of variable benthic nitrogen fluxes on initiation and maintenance of blooms.

Furthermore, since only three shoal stations, 2, 5, and 9, were sampled during both months, this study was limited in detecting temporal variation by a low sample size. This should be avoided in future studies by taking samples at the same stations, preferably including both channel and shoal sites, during each sampling period. Finally, the duration of net flux incubations should be increased. This would allow cores to go anoxic (which would let DNRA and denitrification take place), and increase the accuracy of daily net flux measurements.

References:

- Anderson, I., Tobias, C., Neikirk, B., & Wetzel, R. (1997). Development of a process-based nitrogen mass balance model for a Virginia (USA) *Spartina alterniflora* salt marsh: implications for net DIN flux. *Marine Ecology Progress Series*, 159, 13–27. doi: 10.3354/meps159013
- Anderson, I., Mcglathery, K., & Tyler, A. (2003). Microbial mediation of reactive nitrogen transformations in a temperate lagoon. *Marine Ecology Progress Series*, 246, 73–84. doi: 10.3354/meps246073
- Anderson, I. C., Brush, M. J., Piehler, M. F., Currin, C. A., Stanhope, J. W., Smyth, A. R., ... Whitehead, M. L. (2013). Impacts of Climate-Related Drivers on the Benthic Nutrient Filter in a Shallow Photic Estuary. *Estuaries and Coasts*, 37(S1), 46–62. doi: 10.1007/s12237-013-9665-5
- Brandes, J. A., Devol, A. H., & Deutsch, C. (2007). New Developments in the Marine Nitrogen Cycle. *ChemInform*, 38(20). doi: 10.1002/chin.200720269
- Countway, R. E., Canuel, E. A., & Dickhut, R. M. (2007). Sources of particulate organic matter in surface waters of the York River, VA estuary. *Organic Geochemistry*, 38(3), 365–379. doi: 10.1016/j.orggeochem.2006.06.004
- Friedrichs, C. T. (2009). York River Physical Oceanography and Sediment Transport. *Journal of Coastal Research*, 10057, 17–22. doi: 10.2112/1551-5036-57.sp1.17
- Haas, L. W., Hastings, S. J., & Webb, K. L. (1981). Phytoplankton Response to a Stratification-Mixing Cycle in the York River Estuary during Late Summer. *Estuaries and Nutrients*, 619–636. doi: 10.1007/978-1-4612-5826-1_33
- Hardison, A. K., Anderson, I. C., Canuel, E. A., Tobias, C. R., & Veuger, B. (2011). Carbon and nitrogen dynamics in shallow photic systems: Interactions between macroalgae, microalgae, and bacteria. *Limnology and Oceanography*, 56(4), 1489–1503. doi: 10.4319/lo.2011.56.4.1489
- Helms, J. R., Mao, J., Stubbins, A., Schmidt-Rohr, K., Spencer, R. G. M., Hernes, P. J., & Mopper, K. (2014). Loss of optical and molecular indicators of terrigenous dissolved organic matter during long-term photobleaching. *Aquatic Sciences*, 76(3), 353–373. doi: 10.1007/s00027-014-0340-0
- Lorenzen, C. J. 1967. Determination of chlorophyll and pheopigments: Spectrophotometric equations. *Limnol. Oceanogr.* 12: 343–346.
- Murphy, A. E., Anderson, I. C., Smyth, A. R., Song, B., & Luckenbach, M. W. (2016). Microbial nitrogen processing in hard clam (*Mercenaria mercenaria*) aquaculture

- sediments: the relative importance of denitrification and dissimilatory nitrate reduction to ammonium (DNRA). *Limnology and Oceanography*, 61(5), 1589–1604. doi: 10.1002/lno.10305
- Reay, W. G. (2009). Water Quality within the York River Estuary. *Journal of Coastal Research*, 10057, 23–39. doi: 10.2112/1551-5036-57.sp1.23
- Rizzo, W. M. (1990). Nutrient Exchanges between the Water Column and a Subtidal Benthic Microalgal Community. *Estuaries*, 13(3), 219. doi: 10.2307/1351912
- Sin, Y., Wetzel, R. L., & Anderson, I. C. (1999). Spatial and Temporal Characteristics of Nutrient and Phytoplankton Dynamics in the York River Estuary, Virginia: Analyses of Long-Term Data. *Estuaries*, 22(2), 260. doi: 10.2307/1352982
- Tobias, C., Anderson, I., Canuel, E., & Macko, S. (2001). Nitrogen cycling through a fringing marsh-aquifer ecotone. *Marine Ecology Progress Series*, 210, 25–39. doi: 10.3354/meps210025
- Virginia Institute of Marine Science LYRE Annual Report. (2019). Retrieved from <https://data.ess-dive.lbl.gov/data>
- Virginia Institute of Marine Science LYRE Annual Report. (2019). Retrieved from <https://data.ess-dive.lbl.gov/data>
- Yin, G., Hou, L., Liu, M., Liu, Z., & Gardner, W. S. (2014). A Novel Membrane Inlet Mass Spectrometer Method to Measure $^{15}\text{NH}_4$ for Isotope-Enrichment Experiments in Aquatic Ecosystems. *Environmental Science & Technology*, 48(16), 9555–9562. doi: 10.1021/es501261s

Tables & Figures:

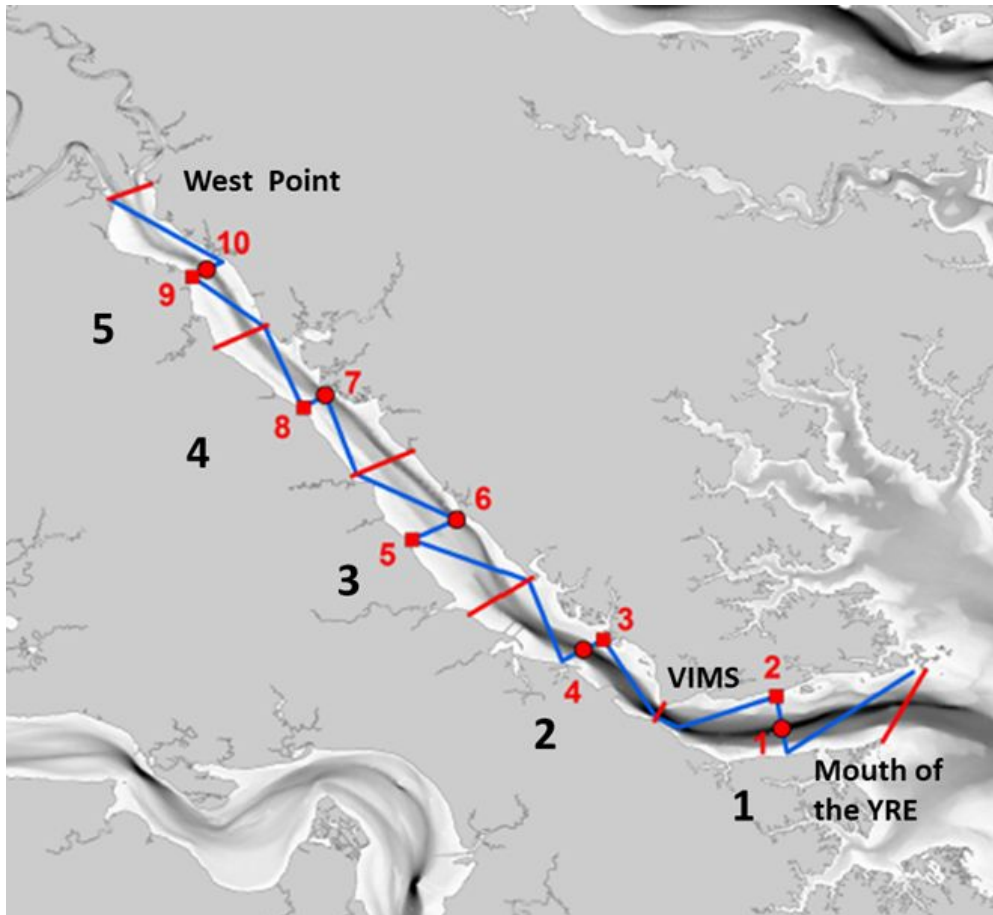


Figure 1: Map of the YRE, with the mouth of the estuary to the right and the head to the left, showing numbered sampling boxes and station locations. The cruise track taken during sampling is shown with the blue line. Sites numbered 1, 4, 6, 7, and 10 are channel stations and numbers 2, 3, 5, 9 are shoal stations (LYRE Annual Report 2019).

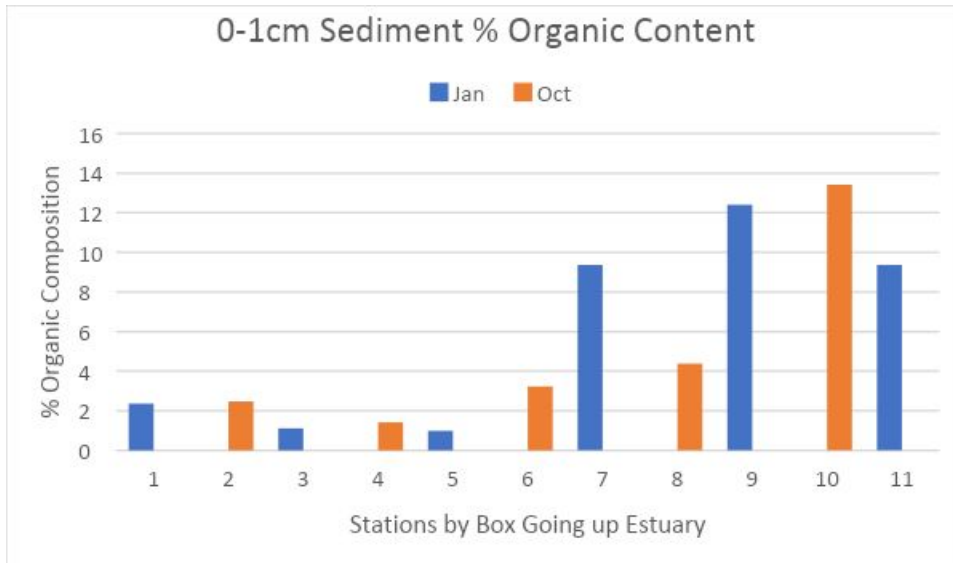


Figure 2: % organic content from the top 1 cm of sediment, grouped by box and station. C represents a channel station; S a shoal station. The different colors represent the months the cores were taken. Box numbers increase going up estuary.

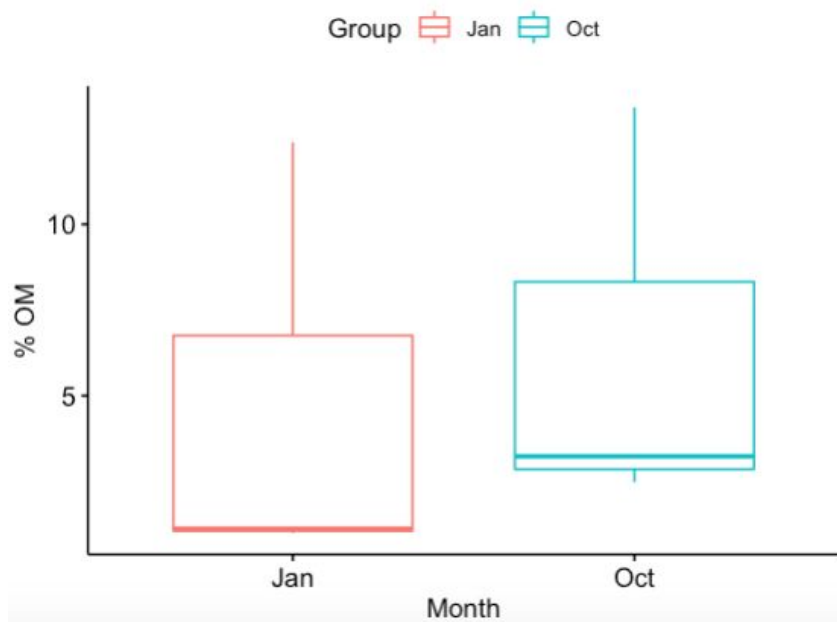


Figure 3: Comparison of sediment % organic matter from stations 2S, 5S, and 9S between January and October. See Table 1 for results of a paired t-test performed on these data. All box and whisker plots in this paper display the median of the data, upper and lower quartiles, maximum and minimums excluding outliers, and outliers.

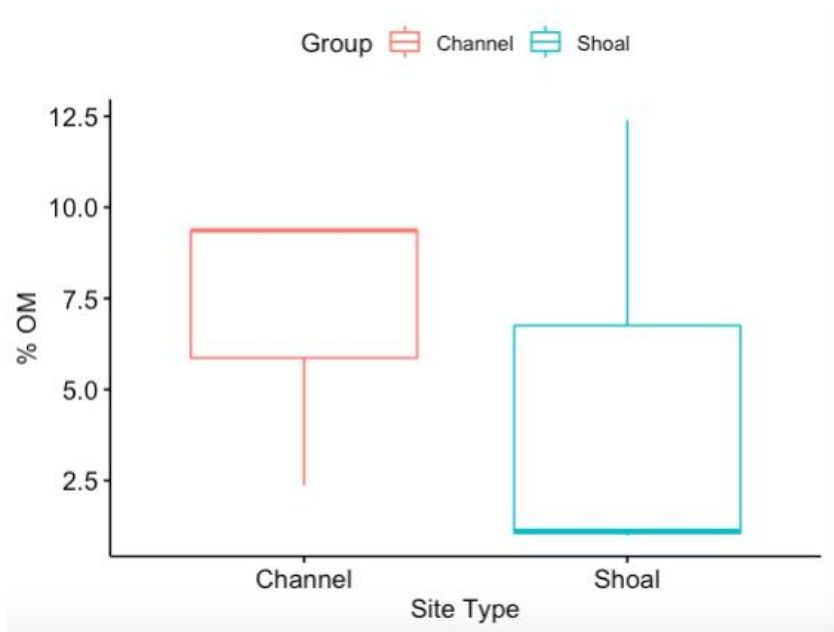


Figure 4: Comparison of sediment % organic matter between shoal and channel stations paired by box. Only January data were used in this comparison since no channel cores were taken in October. See Table 1 for results of a paired t-test performed on these data.

% Organic Matter Paired t-tests					
	df	t-value	p-value	95% confidence interval	mean of the differences
January vs. October	2.00	-4.22	0.05	-3.11 - 0.03	-1.54
Channel vs. Shoal	2.00	0.66	0.58	-12.12 - 16.51	2.20

Table 1: Results of the paired t-tests conducted on sediment % organic matter data. Tests resulting in a p-value <0.05 are colored red. See Figures 3 & 4 for plots of these data.

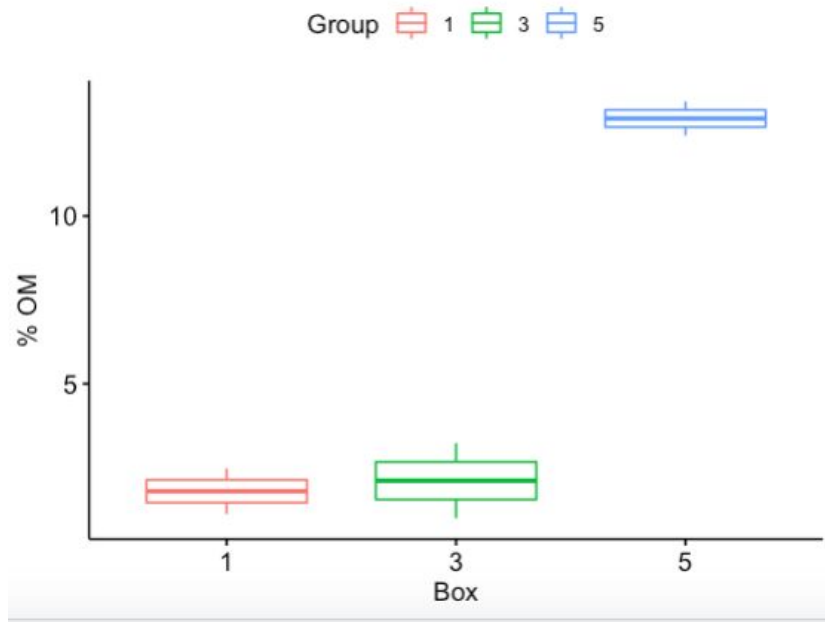


Figure 5: Comparison of sediment % organic matter from stations 2S, 5S, and 9S by box. Box numbers increase going up estuary. See Table 2 for results of an ANOVA comparing these data.

% Organic Content One Way ANOVA by Box			
Box #s Compared	p-value	95% confidence interval	mean of the differences
3-1	0.96	-4.48 - 5.11	0.31
5-1	0.01	6.31 - 15.91	11.11
5-3	0.01	6.00 - 15.60	10.80

Table 2: Results of a one way ANOVA comparing sediment % organic content between sampling boxes. Box numbers increase going up estuary. Comparisons resulting in a p-value <0.05 are colored red. See Figure 5 for a plot of these data.

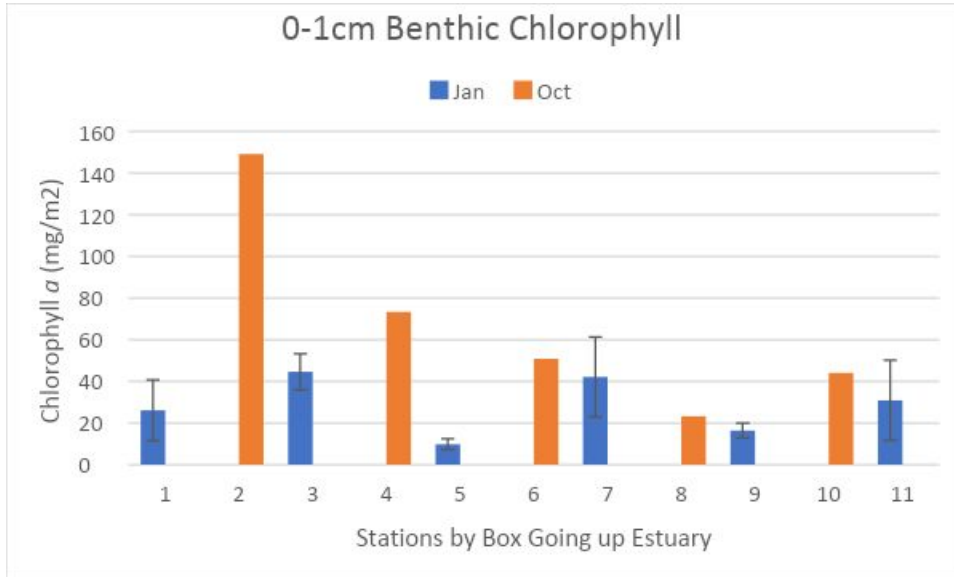


Figure 6: Benthic chlorophyll *a* concentrations from the top 1 cm of sediment, grouped by box and station. The different colors represent the months the cores were taken. Box numbers increase going up estuary. Error bars display standard error.

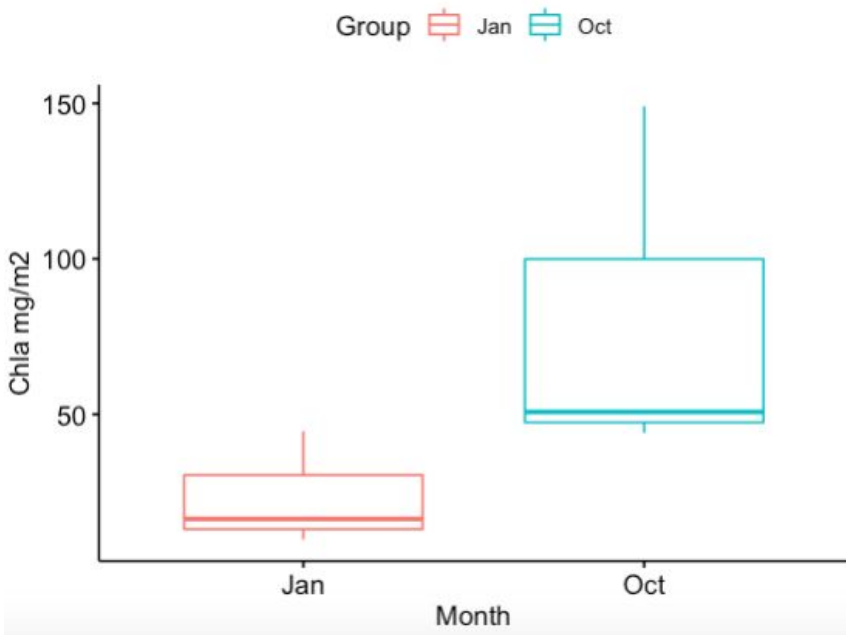


Figure 7: Comparison of chlorophyll *a* concentrations from stations 2S, 5S, and 9S between January and October. See Table 3 for results of a paired t-test performed on these data.

Benthic Chlorophyll <i>a</i> Paired t-tests mg/m ²					
	df	t-value	p-value	95% confidence interval	mean of the differences
January vs. October	2.00	-2.44	0.14	-159 - 44.25	-57.73
Channel vs. Shoal	2.00	0.63	0.59	-54.63 - 73.54	9.46

Table 3: Results of the paired t-tests conducted on benthic chlorophyll *a* data. Tests resulting in a p-value <0.05 are colored red. See Figure 7 for a plot of chlorophyll *a* concentrations in January vs. October.

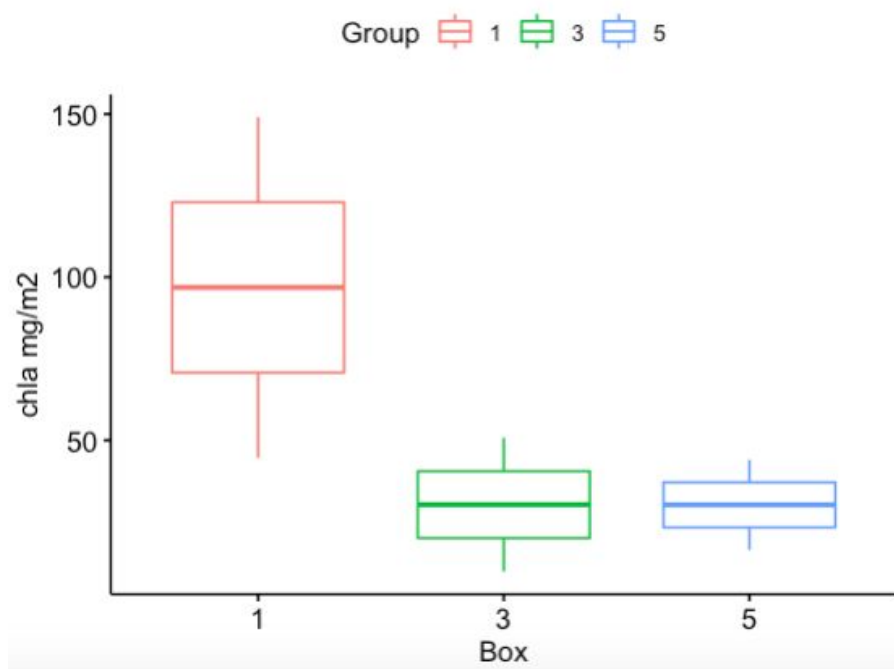


Figure 8: Comparison of chlorophyll *a* concentrations from stations 2S, 5S, and 9S by box. Box numbers increase going up estuary. See Table 4 for results of an ANOVA comparing these data.

Benthic Chlorophyll <i>a</i> One Way ANOVA by Box mg/m ²			
Box #s Compared	p-value	95% confidence interval	mean of the differences
3-1	0.44	-263.86 - 130.69	-66.58
5-1	0.44	-263.92 - 130.62	-66.65
5-3	0.99	-197.34 - 197.21	-0.07

Table 4: Results of a one way ANOVA comparing benthic chlorophyll *a* between sampling boxes. Box numbers increase going up estuary. Comparisons resulting in a p-value <0.05 are colored red. See Figure 8 for a plot of these data.

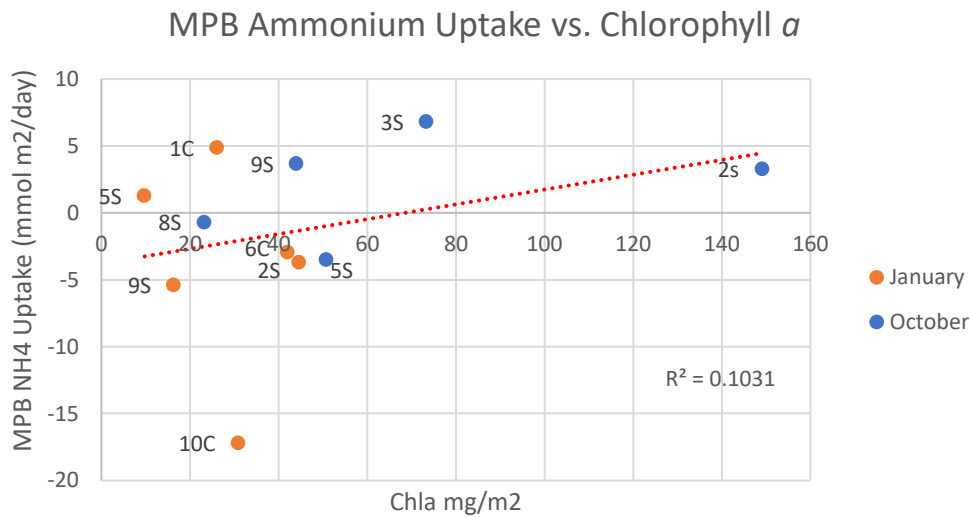


Figure 9: Linear regression of MPB ammonium uptake ($\text{mmol m}^{-2} \text{d}^{-1}$) vs. chlorophyll a concentrations (mg/m^2) colored by month and labeled by station. Trendline, equation, and R^2 on chart are calculated from both months combined. For formulas and R^2 of trendlines by month and combined, see Table 5.

MPB Uptake ($\text{mmol m}^2/\text{day}$) vs. Chlorophyll a (mg/m^2) Linear Regression		
	line of best fit equation	R^2
October	$y = 0.03x - 0.29$	0.15
January	$y = -0.12x - 0.42$	0.05
Both Months	$y = 0.06x - 3.80$	0.1

Table 5: Formulas for the lines of best fit and R^2 values of the linear regressions of MPB ammonium uptake vs. chlorophyll a . See figure 9 for a plot of these data.

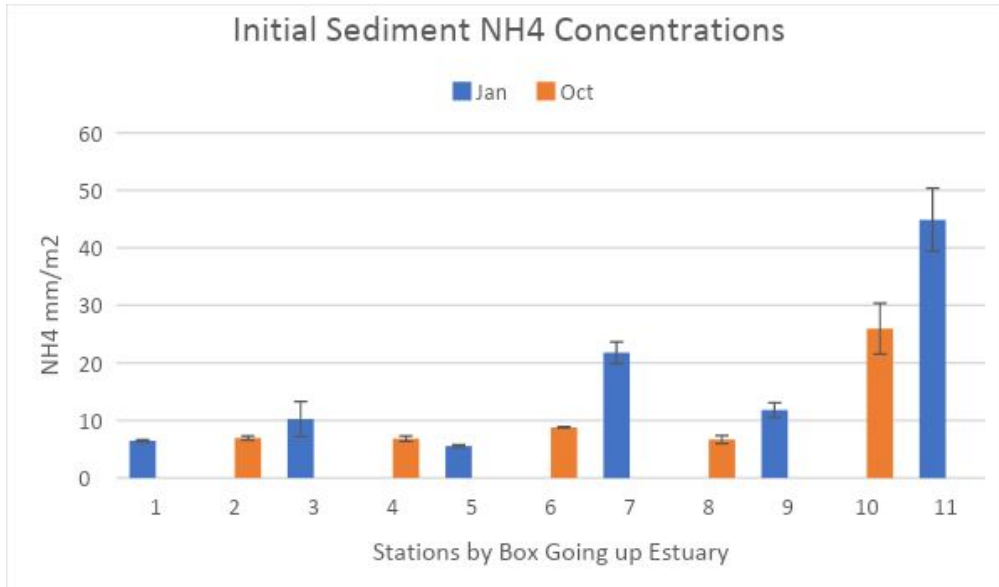


Figure 10: Initial ammonium concentrations grouped by box and station. The different colors represent the months the cores were taken. Box numbers increase going up estuary. Error bars display standard error.

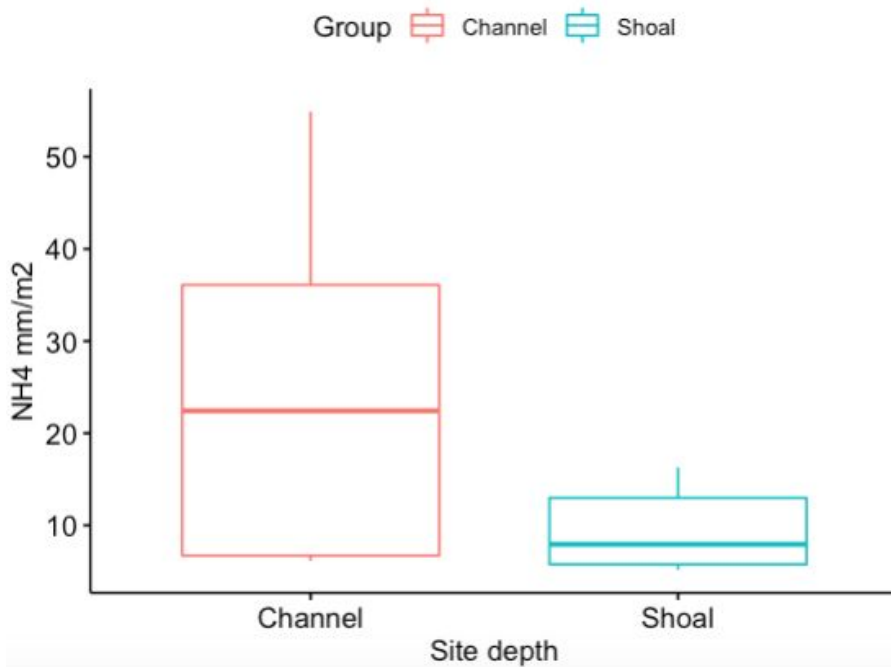


Figure 11: Comparison of initial ammonium concentrations between shoal and channel stations paired by box. Only January data was used in this comparison since no channel cores were taken in October. See Table 6 for results of a paired t-test performed on these data.

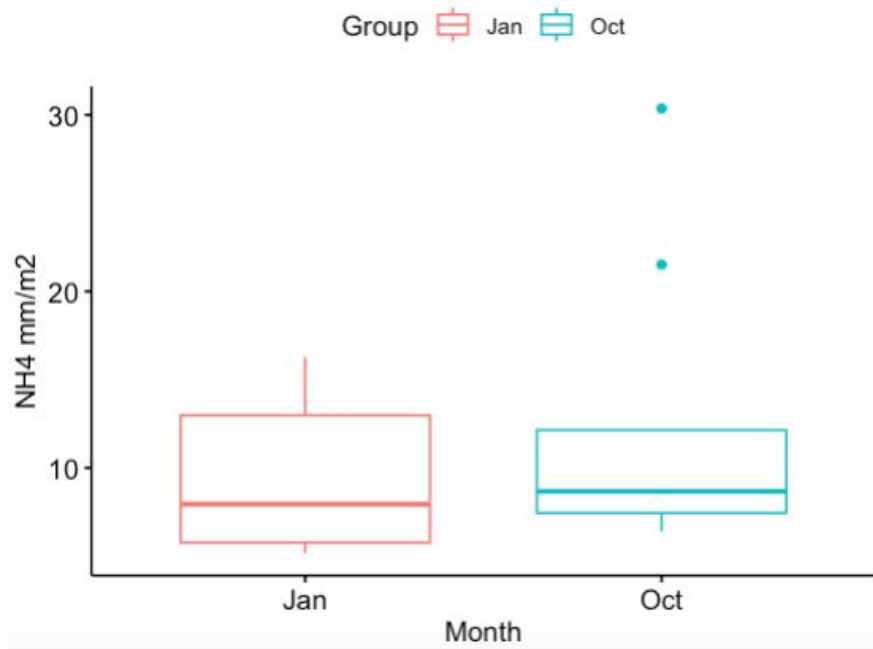


Figure 12: Comparison of initial ammonium concentrations from stations 2S, 5S, and 9S between January and October. See Table 6 for results of a paired t-test performed on these data.

Initial Ammonium Paired t-tests mmol/m2					
	df	t-value	p-value	95% confidence interval	mean of the differences
January vs. October	7.00	-0.67	0.52	-12.41 - 6.91	-2.75
Channel vs. Shoal	8.00	2.72	0.03	2.33 - 28.03	15.18

Table 6: Results of the paired t-tests conducted on initial ammonium concentration data. Tests resulting in a p-value <0.05 are colored red. See Figure 11 and 12 for plots of these data.

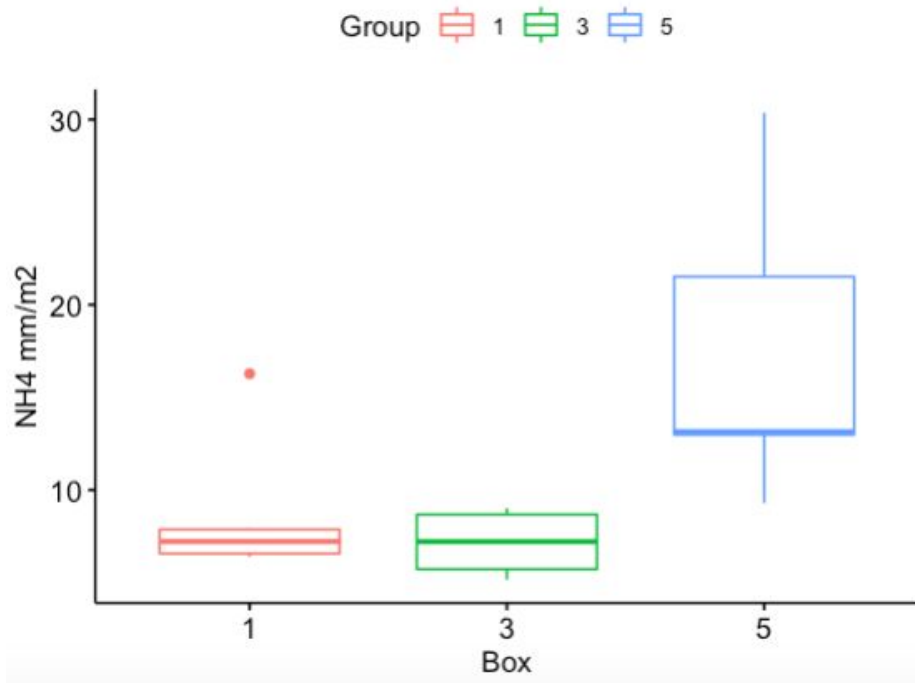


Figure 13: Comparison of initial ammonium concentrations from stations 2S, 5S, and 9S by box. Box numbers increase going up estuary. See Table 7 for results of an ANOVA comparing these data.

Initial Ammonium One Way ANOVA by Box mmol/m2			
Box #s Compared	p-value	95% confidence interval	mean of the differences
3-1	0.88	-9.27 - 6.42	-1.43
5-1	0.03	0.64 - 17.10	8.87
5-3	0.01	2.07 - 18.52	10.30

Table 7: Results of a one way ANOVA comparing initial ammonium concentrations between sampling boxes. Box numbers increase going up estuary. Comparisons resulting in a p-value <0.05 are colored red. See Figure 13 for a plot of these data.

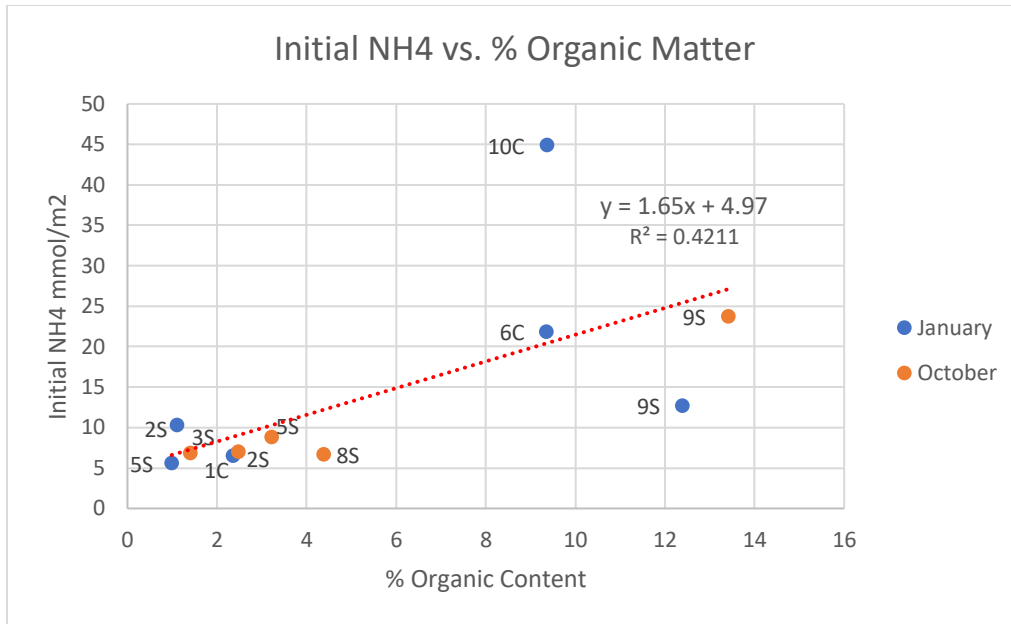


Figure 14: Linear regression of initial sediment ammonium concentration (mmol/m²) vs. sediment % organic content colored by month and labeled by station. Trendline, equation, and R² on chart are calculated from both months combined. For formulas and R² of trendlines by month and combined, see Table 8.

Initial Ammonium (mmol/m ²) vs. % Organic Matter Linear Regression		
	line of best fit equation	R ²
October	$y = 1.48x + 3.20$	0.42
January	$y = 1.68x + 6.99$	0.32
Both Months	$y = 1.65x + 4.97$	0.94

Table 8: Formulas for the lines of best fit and R² values of the linear regressions of initial sediment ammonium vs. sediment % organic content. See Figure 14 for a plot of these data.

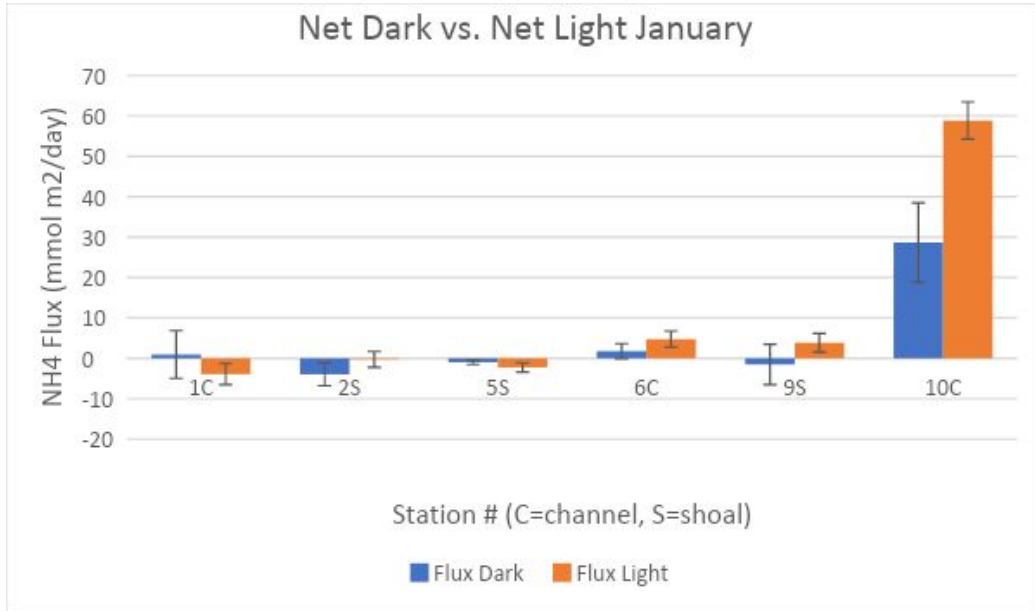


Figure 15: Comparison of net flux rates from dark incubations to net flux rates from light incubations by station in January. The difference is used as the rate of MPB ammonium uptake. Error bars display standard error. Positive fluxes show ammonium release and negative fluxes show uptake by the sediment.

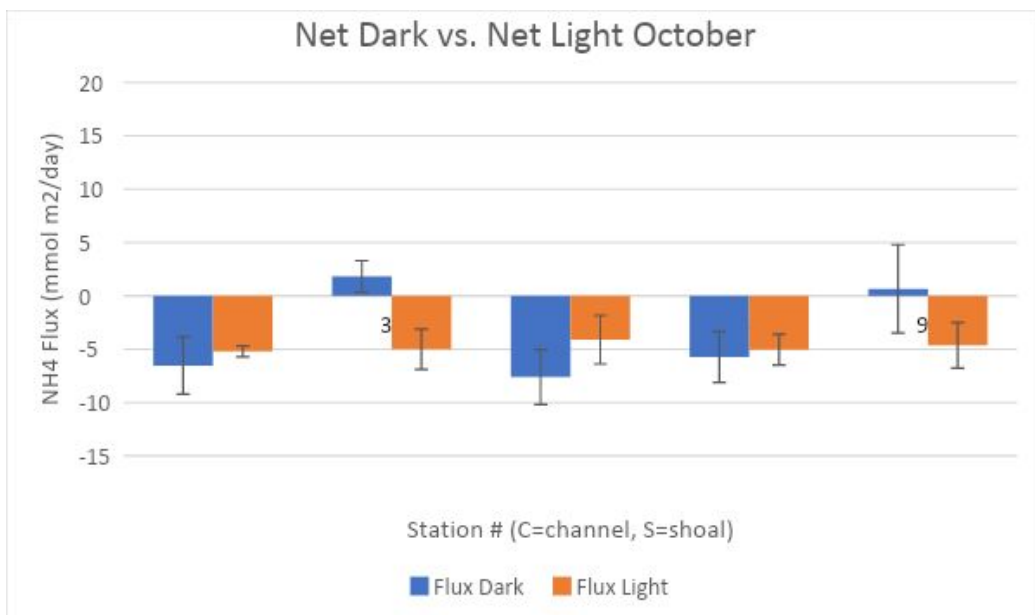


Figure 16: Comparison of net flux rates from dark incubations to net flux rates from light incubations by station in October. The difference is used as the rate of MPB ammonium uptake. Error bars display standard error.

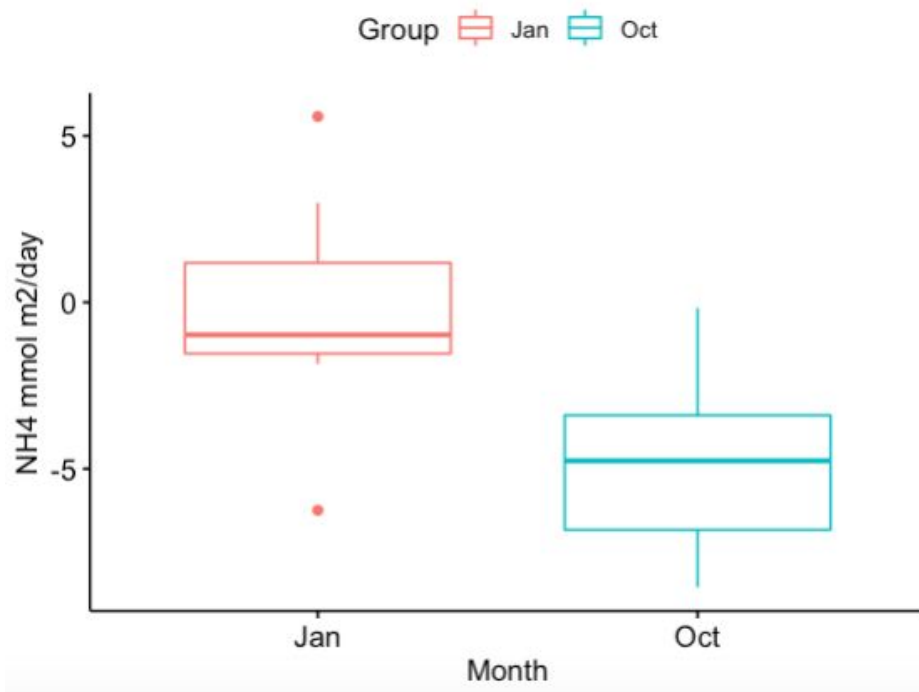


Figure 17: Comparison of net ammonium flux rates from stations 2S, 5S, and 9S between January and October. See Table 9 for results of a paired t-test performed on these data.

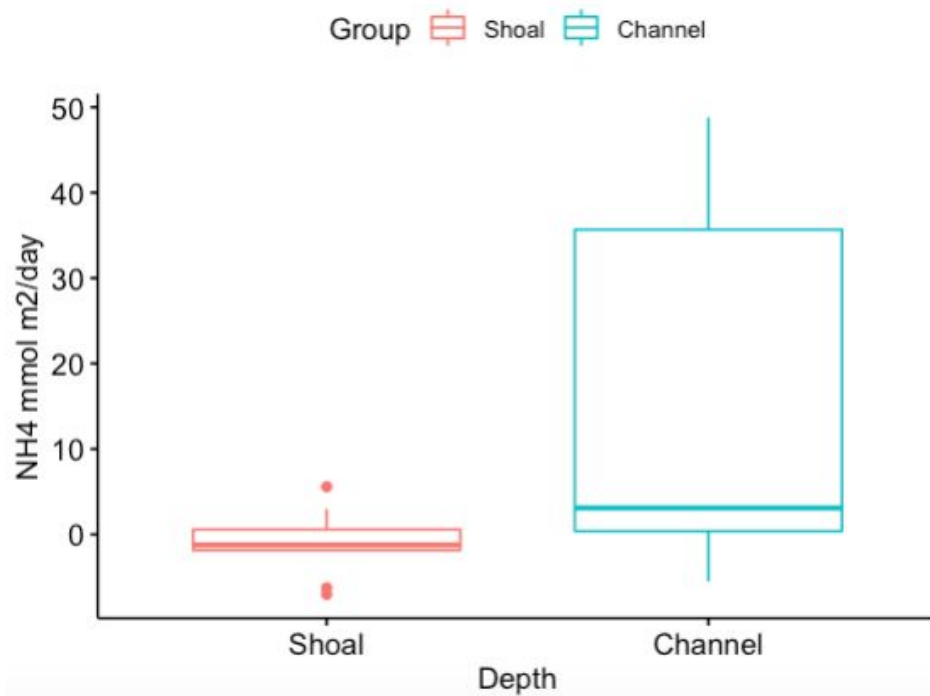


Figure 18: Comparison of net flux rates between shoal and channel stations paired by box. Only January data was used in this comparison since no channel cores were taken in October. See Table 9 for results of a paired t-test performed on these data.

Net Ammonium Flux Paired t-tests mmol m ² /day					
	df	t-value	p-value	95% confidence interval	mean of the differences
January vs. October	7.00	2.57	0.04	0.35 - 8.53	4.44
Channel vs. Shoal	8.00	2.31	0.05	0.04 - 31.01	15.53
January Light vs. Dark	17.00	1.65	0.12	-1.68 - 13.72	6.02
October Light vs. Dark	13.00	-0.70	0.50	-4.76 - 2.44	-1.16
Both Months Light vs. Dark	31.00	1.28	0.21	-1.69 - 7.45	2.88

Table 9: Results of the paired t-tests conducted on net ammonium flux data. Tests resulting in a p-value <0.05 are colored red. See Figures 17 & 18 for plots of January vs. October and Channel vs. Shoal data.

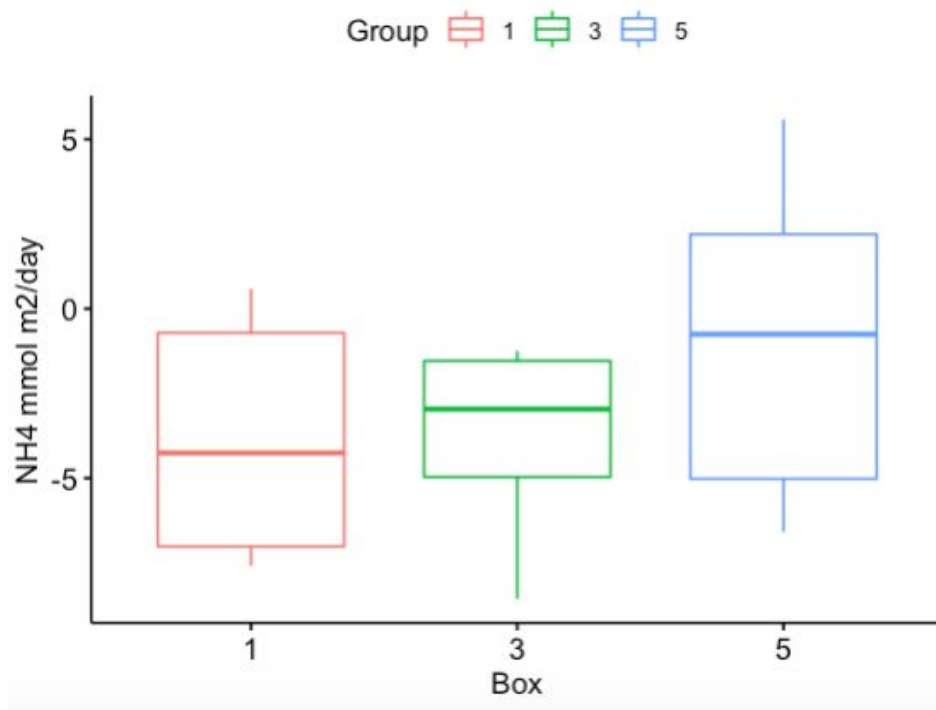


Figure 19: Comparison of net ammonium flux rates from stations 2S, 5S, and 9S by box. Box numbers increase going up estuary. See Table 10 for results of an ANOVA comparing these data.

Net Flux Incubations One Way ANOVA by Box mmol m ² /day			
Box #s Compared	p-value	95% confidence interval	mean of the differences
3-1	0.99	-6.13 - 6.24	0.06
5-1	0.47	-3.35 - 9.02	2.83
5-3	0.45	-3.11 - 8.68	2.78

Table 10: Results of a one way ANOVA comparing net ammonium fluxes between sampling boxes. Box numbers increase going up estuary. Comparisons resulting in a p-value <0.05 are colored red. See Figure 19 for a plot of these data.

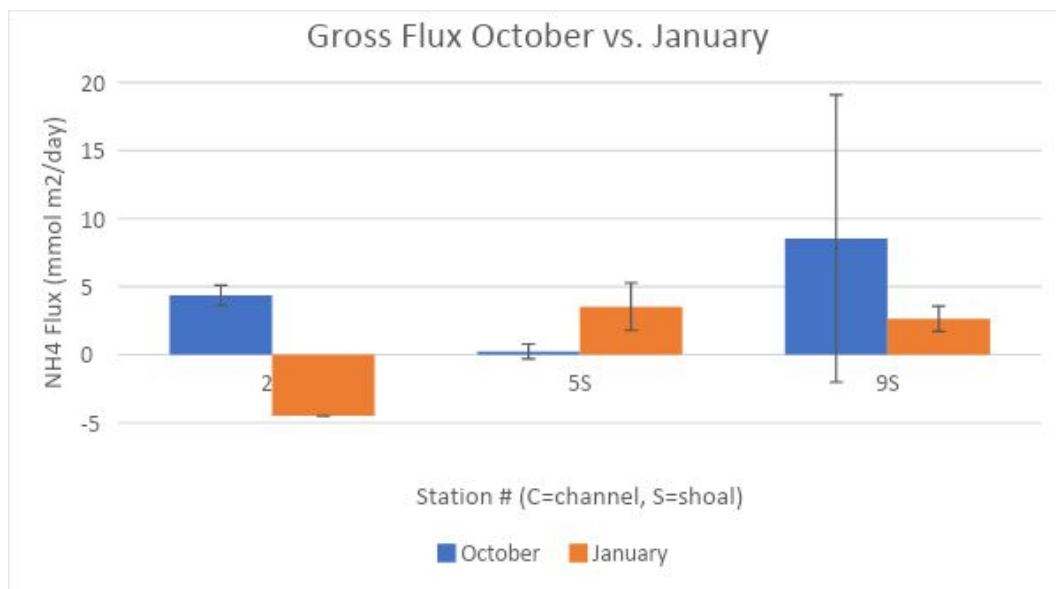


Figure 20: Comparison of gross ammonium fluxes by station between October and January incubations. Error bars display standard error.

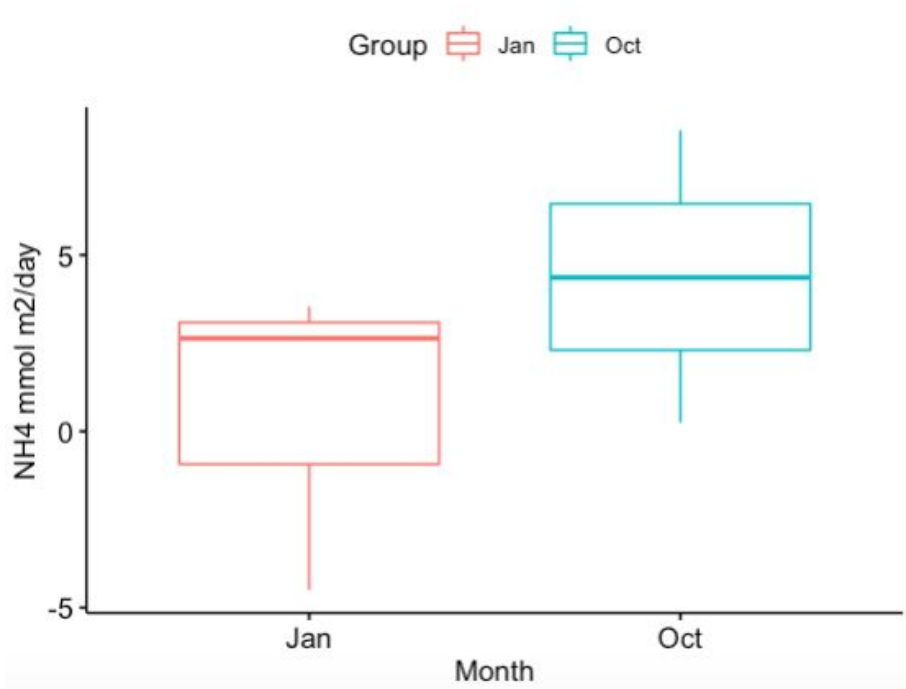


Figure 21: Comparison of gross ammonium flux rates from stations 2S, 5S, and 9S between January and October. See Table 12 for results of a paired t-test performed on these data.

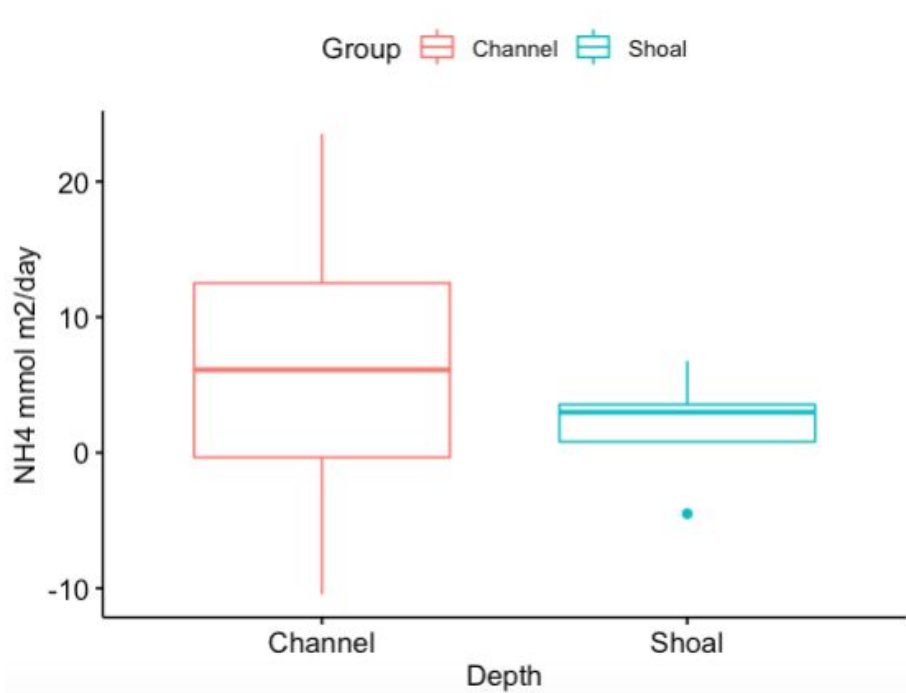


Figure 22: Comparison of gross flux rates between shoal and channel stations paired by box. Only January data was used in this comparison since no channel cores were taken in October. See Table 12 for results of a paired t-test performed on these data.

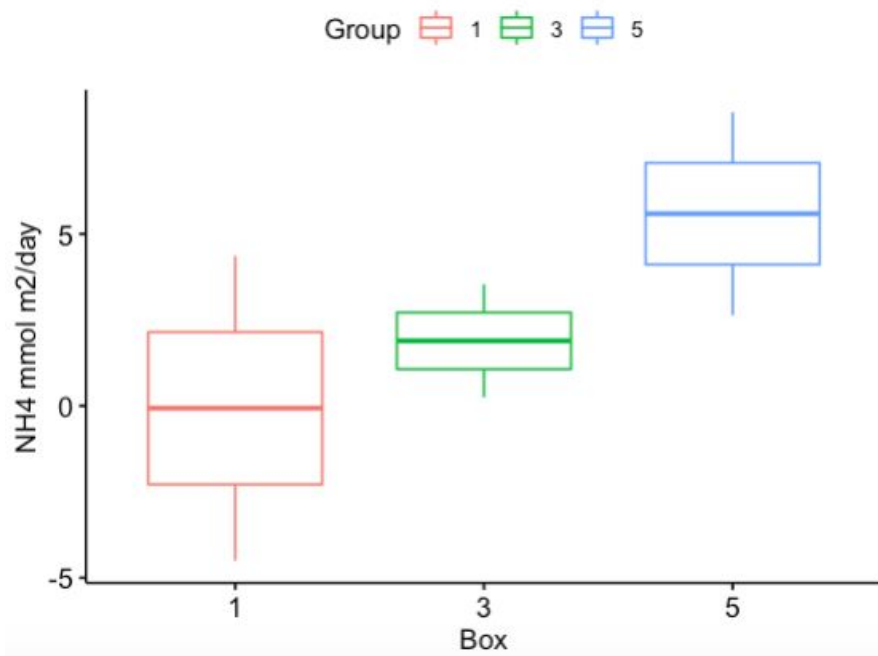


Figure 23: Comparison of gross ammonium flux rates from stations 2S, 5S, and 9S by box. Box numbers increase going up estuary. See Table 11 for results of an ANOVA comparing these data.

Gross Flux Incubations One Way ANOVA by Box mmol m ² /day			
Box #s Compared	p-value	95% confidence interval	mean of the differences
3-1	0.91	-17.05 - 20.97	1.96
5-1	0.51	-13.35 - 24.67	5.66
5-3	0.72	-15.31 - 22.71	3.70

Table 11: Results of a one way ANOVA comparing gross ammonium fluxes between sampling boxes. Box numbers increase going up estuary. Comparisons resulting in a p-value <0.05 are colored red. See Figure 23 for a plot of these data.

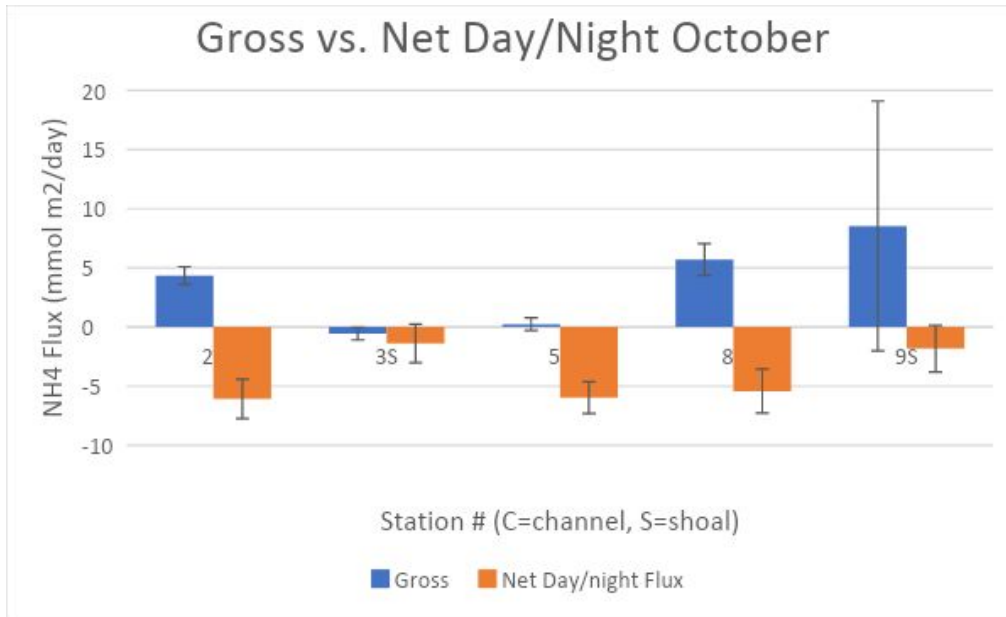


Figure 24: Comparison of gross and net ammonium fluxes by station in October. The difference shows ammonium uptake by either the MPB or nitrifying bacteria. Error bars display standard error.

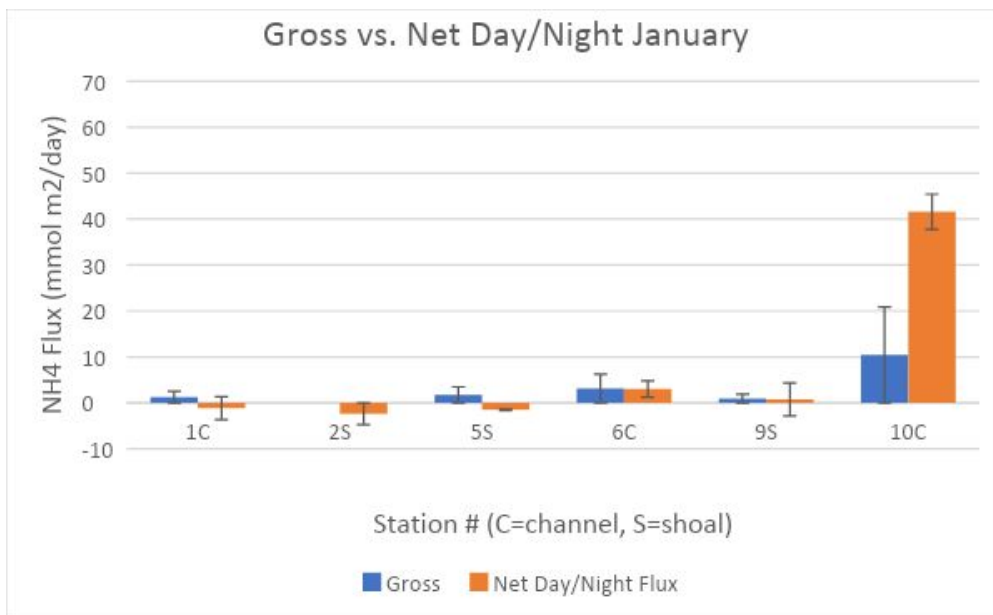


Figure 25: Comparison of gross and net ammonium fluxes by station in January. The difference shows ammonium uptake by either the MPB or nitrifying bacteria. Error bars display standard error.

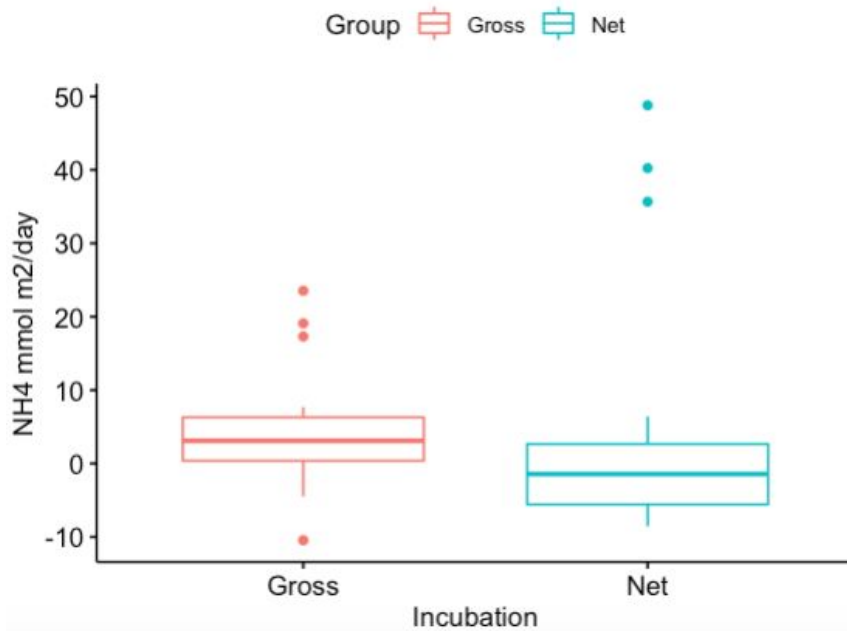


Figure 26: Comparison of gross and net flux rates from October and January combined. See Table 12 for results of a paired t-test comparing these data.

Gross Ammonium Flux Paired t-tests mmol m ² /day					
	df	t-value	p-value	95% confidence interval	mean of the differences
January vs. October	2.00	-1.05	0.41	-19.57 - 11.92	-3.82
Channel vs. Shoal	6.00	1.06	0.33	-5.51 - 13.94	4.22
January Gross vs. Net	15.00	2.11	0.05	-0.09 - 21.16	10.54
October Gross vs. Net	10.00	0.77	0.46	-4.08 - 8.37	2.14
Both Months Gross vs. Net	26.00	0.51	0.61	-4.21 - 6.99	1.39

Table 12: Results of the paired t-tests conducted on gross ammonium flux data. Tests resulting in a p-value <0.05 are colored red. See Figures 21, 22, and 26 for plots of these data.

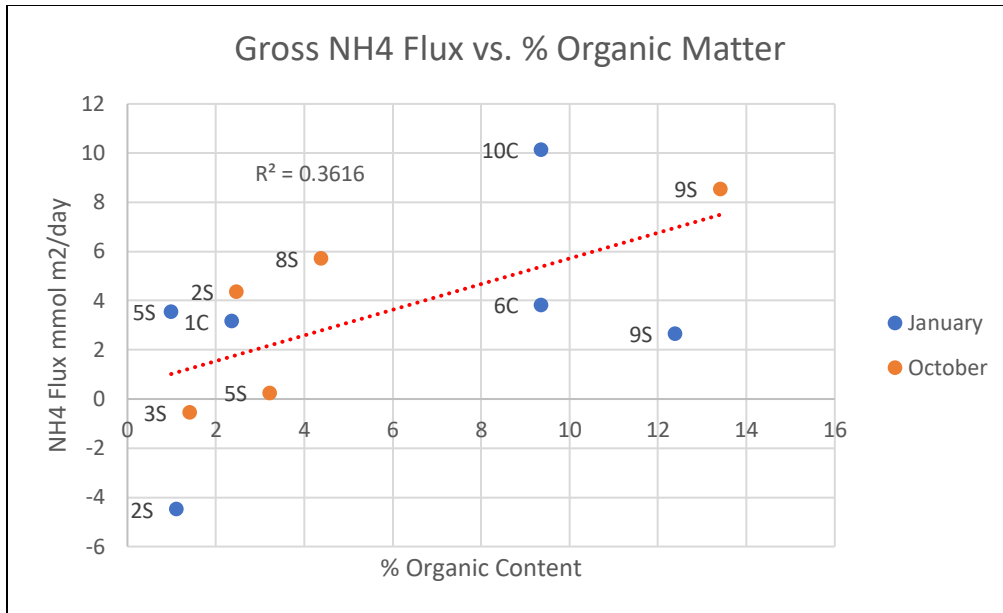


Figure 27: Linear regression of gross sediment ammonium flux (mmol m²/day) vs. sediment % organic content colored by month and labeled by station. The trendline and R² on the chart are calculated from both months combined. For formulas and R² of trendlines by month and combined, see Table 13.

Gross Ammonium Fluxes (mmol m ² /day) vs. % Organic Matter Linear Regression		
	line of best fit equation	R ²
October	y = 0.63x + 0.50	0.65
January	y = 0.46x + 0.40	0.25
Both Months	y = 0.52x + 0.50	0.36

Table 13: Formulas for the lines of best fit and R² values of the linear regressions of gross ammonium fluxes vs. sediment % organic content. See Figure 27 for a plot of these data.